NRC Research Press

ARTICLE

A membrane-spanning macrocyclic bolaamphiphile lipid mimic of archaeal lipids

Gavin M. Mitchell, Amelia Hesketh, Christie Lombardi, Cally Ho, and Thomas M. Fyles

Abstract: The synthesis of a 72-membered macrocyclic tetraester bolaamphiphile is accomplished in six chemical steps from commercially available starting materials using copper-accelerated azide–alkyne coupling to close the macrocycle in high yield. Related diester amphiphiles and an acyclic tetraester bolaamphiphile were also prepared. The set of lipids bearing nitrophenyl phosphate head groups were incorporated into phospholipid vesicles but failed to undergo phosphate hydrolysis in basic conditions, undergoing efficient elimination in competition. The same lipid cores bearing phosphate-linked nitrobenzoxadiazole (NBD) head groups also incorporated into phospholipid vesicles and the NBD fluorescence was quenched with cobalt ions. The proportion of membrane-spanning bolaamphiphiles was determined from the ratio of cobalt quenching in the presence and in the absence of a detergent. The macrocyclic bolaamphiphile is incorporated into phospholipid vesicles such that 48 ± 4% of the NBD head groups are in the outer leaflet, consistent with a membrane-spanning orientation. The acyclic bolaamphiphile is incorporated with 75 ± 3% of the NBD head groups accessible to quencher in the absence of a detergent suggesting U-shaped incorporation in the outer leaflet of the bilayer membrane. In ring size and spanning ability, the macrocyclic bolaamphiphile mimics naturally occurring macrocyclic archaeal lipids.

Key words: macrocyclic lipid, membrane spanning, bolaamphiphile, synthesis, fluorescence, quenching.

Résumé : Nous avons réalisé la synthèse d'un bolaamphiphile, consistant en un tétraester macrocyclique à 72 membres, en six étapes chimiques à partir de produits de départ commerciaux en effectuant la fermeture du macrocycle en rendement élevé au moyen d'un couplage azoture–alcène catalysé par le cuivre. Nous avons également préparé des diesters amphiphiles apparentés et un tétraester acyclique bolaamphiphile. Les lipides de la série portant des têtes constituées de groupes nitrophénylphosphate se sont incorporés dans des vésicules phospholipidiques, mais l'hydrolyse des groupes phosphates en conditions basiques a échoué, et la réaction s'est soldée par une élimination concurrentielle efficace. Les mêmes structures lipidiques, mais dont les têtes étaient constituées de groupes nitrobenzodioxazole (NBD) liés à des groupes phosphate, se sont elles aussi incorporées dans des vésicules phospholipidiques, et une extinction de la fluorescence des groupes NBD a été observée en présence d'ions de cobalt. Nous avons déterminé la proportion de bolaamphiphiles transmembranaires d'après le rapport de l'extinction par le cobalt en présence et en absence de détergent. Le bolaamphiphile macrocyclique s'incorpore dans les vésicules phospholipidiques de sorte que 48 ± 4 % des têtes NBD se trouvent dans la couche externe, ce qui concorde avec une orientation transmembranaire. Le bolaamphiphile acyclique s'incorpore de sorte que 75 ± 3 % des têtes NBD sont accessible à l'extincteur en absence d'un détergent, ce qui semble indiquer une incorporation en forme de « U » dans la couche externe de la bicouche membranaire. Sur les plans de la taille du cycle et de la capacité d'incorporation transmembranaire, les bolaamphiphiles macrocycliques simulent les lipides macrocycliques archéobactériens naturels. [Traduit par la Rédaction]

Mots-clés : lipide macrocyclique, transmembranaire, bolaamphiphile, synthèse, fluorescence, extinction.

Introduction

The lipids of species of the domain *Archaea* are distinct from those of eukaryotes and bacteria.[1,2] Alhough the lipids of the latter two domains are largely fatty acid-derived esters of *R*-1,2-glycerol-phosphoesters, archaeal lipids are terpene-derived ethers of *S*-1,2-glycerol with the 3-position bearing either a phospho- or a glyco-linked head group (Fig. 1). Whatever their role in early evolution,[3] modern *Archaea* species occupy harsh environments; extreme halophiles live in warm high-salt brines, thermoacidophiles require hot acidic environments, and extreme thermophiles grow optimally at temperatures above 80 °C.[1,2] The common assumption is that the chemical composition of the lipid membranes of *Archaea* facilitates survival in extreme conditions through the additional chemical stability of hydrolysis-resistant ether linkages in the lipid core (Fig. 1). Additionally, archealipids contain apparent tail-to-tail dimer lipids based on a macrocyclic caldarchaeol lipid core. The hydrocarbon segments of the caldarchaeols can be diphytane-α,ω-diols or are additionally oxidized to incorporate up to eight *trans*-1,3-cyclopentano units.[1,2] Caldarchaeol-derived lipids are bolaamphiphiles bearing two polar head groups bridged by a significant nonpolar region.[4] As such, they are potentially capable of spanning a bilayer composed of single-headed archaeal lipids, and there is evidence that membrane spanning occurs.[5] Another common assumption is that the membrane-spanning components impart additional mechanical stability to the bilayer membranes of *Archaea*.[1,2]

Received 24 May 2016. Accepted 3 July 2016.

G.M. Mitchell, A. Hesketh, C. Lombardi, C. Ho, and T.M. Fyles. Department of Chemistry, University of Victoria, Box 1700 STN CSC, Victoria, BC V8W 3V6, Canada.

Corresponding author: Thomas M. Fyles (email: tmf@uvic.ca).

This paper is part of a Special issue to honor Professor Reginald Mitchell.

Copyright remains with the author(s) or their institution(s). Permission for reuse (free in most cases) can be obtained from RightsLink.

Fig. 1. The lipid structures of *Archaea* differ from those of eukaryotes in the presence of the opposite glycerol stereochemistry, ether linkages, saturated terpenoid hydrocarbon tails, and macrocyclic lipid cores. The proposed archaeal lipid mimic is a hybrid based on a macrocyclic tetraester.

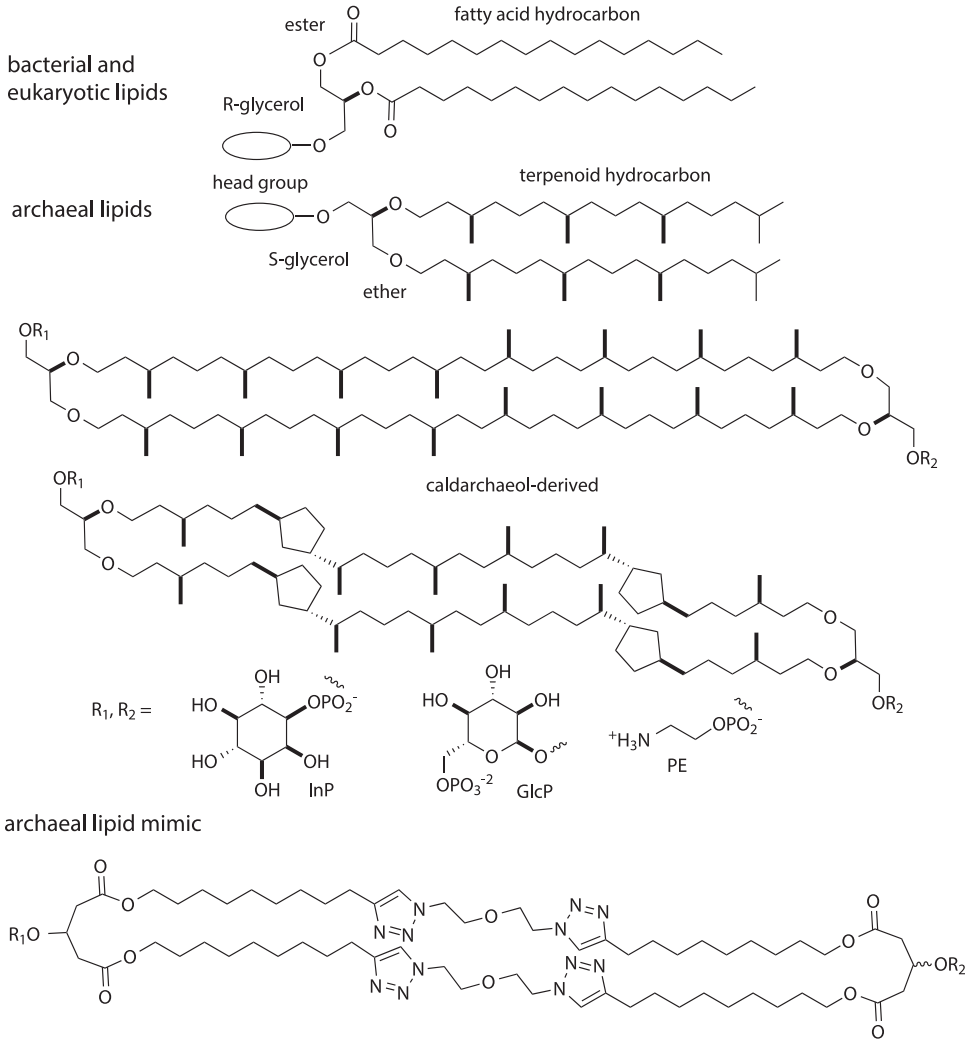

The combination of properties presented by archaeal lipids leads to potential biotechnology applications.[2,6] Liposomes from natural archaeal lipids, known as archaeosomes, are more physically stable than conventional liposomes based on ester-linked phospholipids.[7,8] In particular, archaeosomes are thermally resistant and can maintain entrapment integrity even when autoclaved.[9] Archaeosomes are also more susceptible to uptake by phagocytic cells than liposomes of ester phospholipids,[10] leading to their utility as adjuvants in the development of antibodies.[2,11,12] The wider use of archaeosomes is directly limited by availability of archaeal lipids derived as mixtures from natural sources.[7] The remarkable total synthesis of the 72-membered macrocyclic tetraether archaeal lipid core[13] is lengthy and does not readily lend itself to scale up or to the preparation of lipids with head-group dissymmetry, as commonly found in naturally derived samples.[2,6,7]

Synthetic bolaamphiphiles proposed as archaeal lipid mimics have been explored for over three decades.[4,14,15] Synthetic mimics can offer pure samples of defined structures, but essential structural simplifications to facilitate synthesis also loosen the bounds of mimicry and may result in substantially different functions. Early work focussed on macrocyclic bolaamphiphiles bearing short (C_{12}–C_{18}) spans that produced much thinner monolayer membranes where it is clear that the macrocycles must be membrane-spanning.[16] An alternative approach involves bolaamphiphiles with a single long hydrophobic strand (about 3 nm) separating two head groups.[14,17,18] It is not clear in these cases that the bolaamphiphile is membrane-spanning when mixed with bilayer-forming phospholipids, and U-shaped insertion is common.[18,19] U-shaped insertions of linear strands are associated with enhanced membrane permeability,[19,20] but spanning insertions are uncorrelated with permeability enhancement: some do, others do not.[18,21] Naturally derived archaeal lipids do not necessarily adopt spanning conformations and may also adopt U-shaped organization in films and vesicles,[7,22] which may also influence the water and ionic permeability of archaeosomal membranes.[23] The fine balance between spanning and U-shape in bolaamphiphiles based on a single long strand appears to be related to lipid-packing considerations, albeit in single-component films and aggregates.[15,17,24,25]

From a biotechnology perspective, applications based on pure single-component archaeal lipid mimics are unlikely; mixtures with additional lipid components will be required to control particle size, charge, storage stability, and off-target effects including toxicity.[26,27] In such a lipid-based delivery system, the archaeal lipid mimic would be a minor component designed to provide mechanical stabilization of bilayers predominantly composed of ester-linked phospholipids. It is therefore critical to initially establish that candidate archaeal lipid mimics are miscible in phospholipid bilayers and adopt a membrane-spanning orientation without enhancing membrane permeability. Thereafter, it will be

Scheme 1. Synthetic routes to the lipid cores of acyclic and macrocyclic esters.

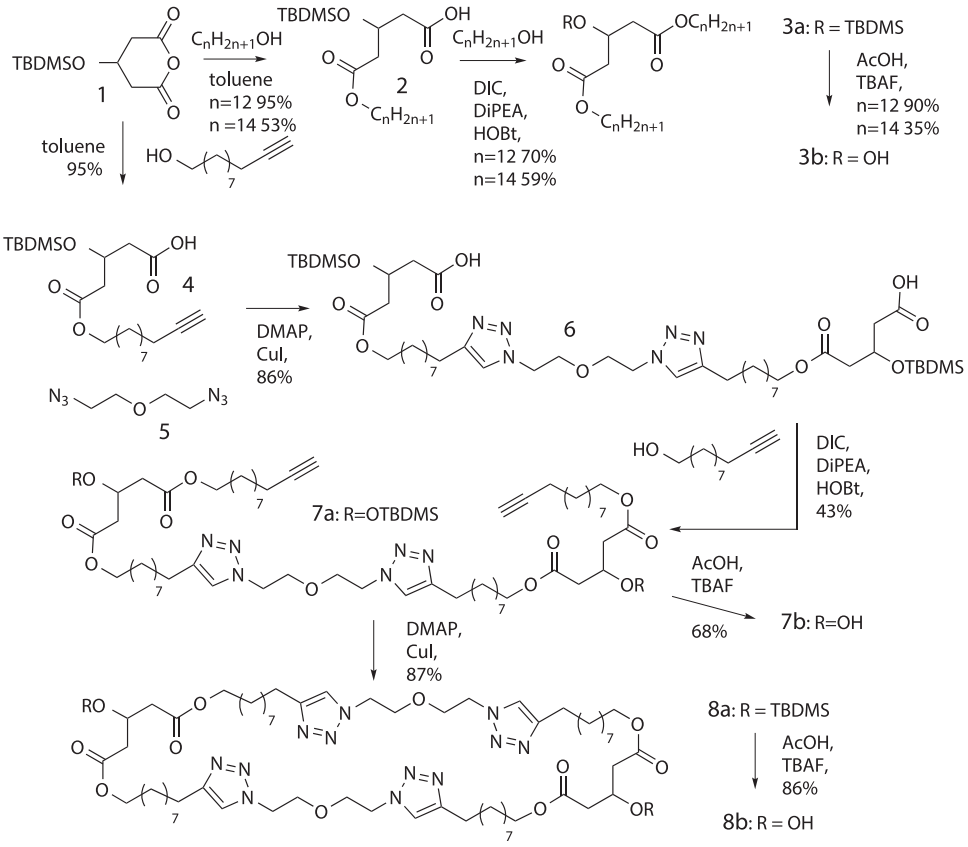

possible to establish if the mimic does impart the expected mechanical stabilization of the lipid mixture formulated for the particular application and thus result in any subsequent benefits related to the archaeal lipid mimic.

Our potential membrane-spanning macrocyclic archaeal lipid mimic is given in Fig. 1. The design is driven by a combination of practical considerations and experience derived from linear oligoester ion channels.[19,20,28–31] Good phospholipid miscibility is associated with extended alkyl esters,[32,33] and the use of glutarate diesters in place of glycerol diesters is both a reliable and simplifying synthetic strategy.[28,34] The 1,2,3-triazole produced via copper-catalyzed alkyne–azide coupling (CuAAC)[35] also has good lipid miscibility in conjunction with esters elsewhere in the structure[33] and has previously featured in single-chain archaeal lipid mimics designed to enhance membrane permeability via flip–flop, which necessarily requires a U-shaped insertion.[36,37] Membrane-inactive per-substituted cyclodextrins bearing triazoles and esters[38] suggest that there is no inherent membrane destabilizing character to triazoles or esters, provided that U-shaped insertions can be avoided. The high reaction rate and efficiency and the potential for Cu-centred templation in CuAAC have been widely exploited in macrocyclizations.[39–41] The target macrocycle is potentially derived from a commercially available bisazide and 10-undecyn-1-ol, the longest commercially available ω-hydroxy alkyne, which coincidentally gives an estimated extended hydrophobic strand length of 3.5 nm — well suited to the requirements of a phospholipid bilayer. Also coincidentally, the mimic contains a 72-membered ring as in the caldarchaeols.

The goal of this study was to explore the synthesis of the potential membrane-spanning macrocycle proposed in Fig. 1 and to establish if it is both miscible and membrane-spanning in a phospholipid bilayer vesicle. Related compounds were also prepared to assist with the development of the synthesis and of the assay for membrane-spanning proportion.

Results and discussion

Synthesis

The synthesis of macrocyclic diol **8b** and related compounds is given in Scheme 1. The protected 3-hydroxyglutarate monoester of 10-undecyn-1-ol was readily prepared using a small excess of the anhydride **1** to drive the process. Compound **4** is unstable in solutions containing any protic solvent, reverting to starting materials, so chromatographic purification was not possible. A procedure involving removal of excess **1** by low-temperature crystallization proved effective. Purifications of previous glutarate monoesters of this type also relied on differential solubility, but of the product monoester not the anhydride.[28,31] The same procedure produced compound **2** from 1-dodecanol (n = 12) or 1-tetradecanol (n = 14), albeit in lower yields due to different product solubility under the low-temperature crystallization conditions.

The first of the projected CuAAC reactions of alkyne **4** with bisazide **5** required extensive optimization of solvent, base, copper source, time, and temperature.[42] A key variable appeared to be the base — dimethylaminopyridine in the optimized protocol — as other bases lead to incomplete reaction, ester cleavage, or deprotection to various degrees. Close control of the 2:1 stoichiometry allowed isolation of product **6** solely by extractive workup. Compound **6** is a very sticky material that readily entraps solvent, which must be removed at high vacuum. Diacid **6** was then converted to the tetraester **7a** using a previously developed esterification protocol[29] for similar glutarate diesters. The same protocol produced **3a** from **2** in variable yields related to purification losses.

Scheme 2. Synthetic routes to nitrophenyl phosphate and nitrobenzoxadiazole phosphate derivatized lipid cores.

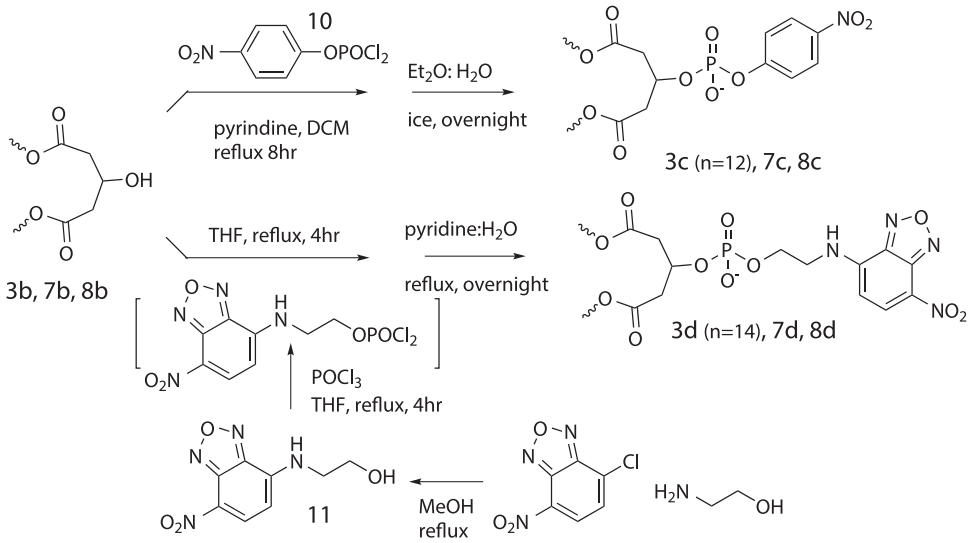

Finally, the diyne **7a** was subjected to the optimized CuAAC conditions with **5** to produce macrocycle **8a** in a remarkable yield of 87%. A key parameter in this reaction was the final concentration (0.11 mol/L product); at higher concentrations some product appeared to be formed but occurred in a poorly soluble and intractable gel[43] containing Cu(II) as judged from a pale blue colour in air-exposed samples, whereas, at a low concentration, the product did not form fast enough to compete with side reactions. Samples contaminated with Cu(II) gave poor NMR spectra, with multiple triazole signals in both ^{1}H and ^{13}C NMR spectra suggesting that a component of the good macrocyclization yield was related to Cu templating. Extensive extraction with EDTA during workup was required to produce clean samples of **8a**, freely soluble in chloroform, with the expected NMR spectra and mass spectrum identified as that of a sodium adduct molecular ion.

Deprotection using TBAF – acetic acid afforded the diol **8b** in apparently quantitative yield, with losses related to purification only. The same protocol produced **3b** from **3a** and **7b** from **7a**. Analysis of incomplete reaction mixtures by ESI-MS provided further evidence that the product from **8a** was the expected macrocycle, because only three species were detected corresponding to the Na^+ adducts of **8a** (1459.95 *m*/*z*), **8b** (1231.80 *m*/*z*), and the intermediate mono TBDMS species (1346.86 *m*/*z*). Had the starting **8a** contained a proportion of oligomers hidden in the complexities of the NMR spectra, these would have produced additional intermediate partially cleaved structures that would have shown additional ESI-MS signals. Compound **8b** is available in 26% yield over five steps from the starting anhydride **1**.

Conversion of the core lipids **8b**, **7b**, and **3b** to amphiphiles requires that polar head groups be appended. A reported assay for membrane-spanning proportion (discussed in the following) uses a nitrophenyl phosphate head group; therefore, the first series of compounds was prepared using 4-nitrophenyl phosphorodichloridate (**10**) to form the phosphate diesters **3c** (*n* = 12), **7c**, and **8c** after pyridine–water hydrolysis (Scheme 2).[44] The amphiphiles are poorly soluble in pure solvents, but adequately soluble in 5% methanol in dichloromethane. Chromatographic losses are significant; therefore, the products were isolated and purified by a dissolution–precipitation sequence to remove excess reagents. The NMR spectra of these products are broadened, but the integrations in the ^{1}H NMR spectra are consistent with the assigned structures. The ESI-MS spectra of compounds **3c** (*n* = 12) and **7c** show the expected $(M–H)^-$ and $(M–2H)^{2-}$ ions. The ESI-MS spectra of **8c** under various conditions are more complex as the monomer ions $(M–2H)^{2-}$ co-occur with dimeric $(2M–4H)^{4-}$ and trimeric $(3M–6H)^{6-}$ ions (Fig. 2).

Fig. 2. Isotope distribution patterns of the molecular ions of **8c** aggregates by high-resolution ESI-MS (negative ion). Triangles, $(M–2H)^{2-}$; squares, $(2M–4H)^{4-}$; circles: $(3M–6H)^{6-}$. [Colour online.]

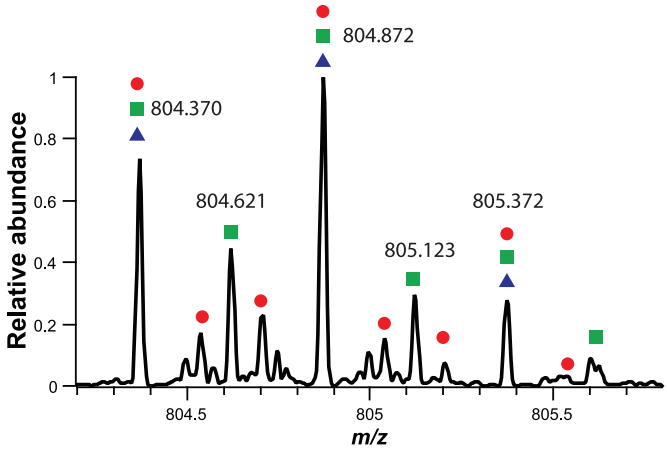

The monoisotopic parent ions of these species occur at the same *m*/*z* (804.370), but the differing charges produce different isotopic patterns that allow the species to be identified. This is further evidence of the macrocyclic bolaamphiphile structure assigned.

Alternative lipids required for a fluorescence-quenching assay of membrane-spanning proportion (see the following) were prepared from the lipid cores **8b**, **7b**, and **3b** using a phosphorodichloridate reagent prepared in situ from **11** and $POCl_3$, which was followed by pyridine–water hydrolysis to give the nitrobenzoxadiazole lipids (NBD-lipids) **8d**, **7d**, and **3d** (*n* = 14) (Scheme 2). The procedure was optimized to utilize reagents in excess to fully convert small amounts of the lipid cores (<10 μmol) to the required compounds, in part to deal with the limited amounts of material then available, and in part to deal with the very gummy insoluble products produced when the solvent was removed. The gummy state could not be redissolved in organic solvent mixtures after it had formed. Gummy samples could be dispersed into aqueous solution, consistent with the formation of lipid aggregates; these were not further explored. Compound characterization of **8d**, **7d**, and **3d** (*n* = 14) rests entirely on the observation of the expected molecular ions in the ESI-MS (negative ion) spectra of the products produced by the protocol as solu-

Fig. 3. Assays to assess membrane-spanning proportion by bolaamphiphile lipids. (A) Schematic of the nitrophenolate release assay.[44] Addition of base results in hydrolysis of phosphate esters on the external face of the vesicle to release a portion of the total nitrophenolate associated with the vesicle; triton addition results in lysis to expose the internal face of the vesicles to the base and results in additional nitrophenolate release. (B) Schematic of the nitrobenzoxadiazole (NBD)-quenching assay. Addition of a quencher to the vesicles results in partial quenching of the total NBD emission proportional to the fraction of externally bound NBD. Addition of triton results in vesicle lysis to expose NBD initially held inside the vesicle and results in quenching of a larger proportion of the total emission. (C) NBD-emission spectra for vesicles containing **8d** (0.2 wt%) showing changes owing to addition of 0.2 mmol/L $CoSO_4$ and triton (excess with respect to total lipid). [Colour online.]

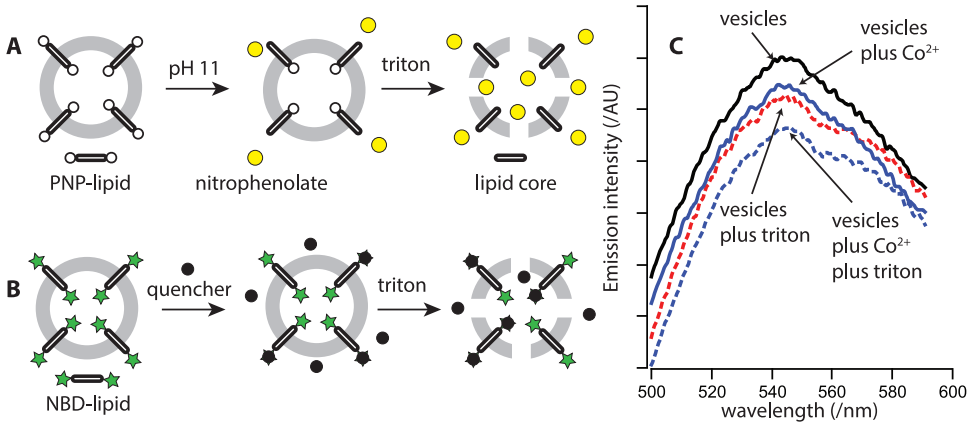

tions of 0.1–1 mmol/L concentration in chloroform and on the expected UV–vis and fluorescence spectra obtained.

Determination of membrane-spanning proportion

Determination of membrane-spanning proportion in a bilayer-membrane vesicle requires a technique to differentiate those head groups of a bolaamphiphile that reside in the outer leaflet from those located on the inner leaflet. This requires a surface-specific reaction by a membrane-impermeable reactant (Fig. 3A). The pioneering work by Moss and co-workers exploited base-promoted ester hydrolysis to expose a nitrophenolate ion from the head groups of a single-strand bolaamphiphile in vesicles composed of quaternary ammonium lipids; a "rapid" phase of the reaction over the first 100 s produced 50% of the eventual (8 h) total nitrophenolate produced.[45] This was taken as evidence that the bolaamphiphile was exclusively membrane-spanning in the initial stages of the reaction. The same strategy of surface-specific reaction was exploited to create transverse asymmetric lipid distributions[44,46] as a prelude to examining lipid flop–flop rates. The observation of 50% surface reaction in this type of assay does not rule out the possibility that the bolaamphiphiles are also inserted as U-shaped within a single leaflet, with equal proportions on the inner and outer leaflets, and subsequent control experiments on flip–flop rates are required to rule out this possibility.[45]

As discussed previously, a commercially available reagent readily converted the lipid cores to suitable nitrophenylphosphate ester amphiphiles **3c** ($n = 12$), **7c**, and **8c** needed to utilize the Moss assay for membrane-spanning proportion.[44] Mixed lipid films of L-α-phosphatidylcholine containing about 1 mol% of **3c** ($n = 12$), **7c**, or **8c** were hydrated in a phosphate buffer at pH 6.4, and vesicles of diameter 125–150 nm were formed using a conventional sequence of cycles of freeze–thaw, sonication, extrusion sizing, and gel filtration for all three additives. Despite the apparent incorporation of **3c** ($n = 12$), **7c**, or **8c** into the vesicles, a shift in pH to 11.8 by addition of NaOH failed to release any of the expected yellow nitrophenolate ion in any attempt. There are several possibilities for this disappointing outcome: the synthetic lipids were not taken into the vesicles during formation or were lost on the gel permeation column; the head group phosphodiester is unreactive under the conditions of the assay; or there is a competing side reaction that does not involve formation of nitrophenolate.

Uptake of **3c** ($n = 12$) or **7c** during vesicle formation was readily established. Vesicles were formed as previously described, triton was added to lyse the vesicles, and the sample was diluted in methanol for ESI-MS (negative ion) analysis. In addition to many peaks related to the other components in this mixture, the expected $(M–H)^-$ ion of **3c** ($n = 12$) was observed at m/z 684.5 and of **7c** at m/z 1454.1 in their respective vesicle samples. Compound **8c** could not be directly detected by this procedure. As noted previously, the observed ions in pure samples include homoaggregates that are not present in the complex spectra obtained. We assume that some of the observed ions are aggregates of **8c** with phosphatidylcholines, but there is no unambiguous assignment of the presence **8c**.

The stability of **3c** ($n = 12$) or **7c** under the reaction conditions was assessed using the same direct ESI-MS analysis of vesicle products following various times of exposure to pH 11.8. We anticipated a decay of the observed parent ions initially present. Given the complexity of the spectra and the relatively crude sample preparation method, it was difficult to establish if there was a time-dependent loss of ion intensity; the molecular ions were observed for both systems under all base treatment times. Both systems did produce new ions on base treatment, and, significantly, both systems produced a new ion 219 mass units lower than the parent (m/z 465.9 from 684.8 for **3c** ($n = 12$) and m/z 1235.1 from 1454.1 for **7c**). This mass difference corresponds to the loss of the entire nitrophenyl phosphate head group without cleavage of the nitrophenyl ester. This suggests that a side reaction occurred by elimination as illustrated in Scheme 3. We expected direct hydrolysis (path following a); we appear to have observed elimination (path following b). A monoanionic species was observed by ESI-MS in both cases. For **7e**, we can assume the remaining phosphate was deprotonated, and the α,β-unsaturated ester is a neutral; however, for **3e** ($n = 12$), we require the additional assumption that the α,β-unsaturated ester is γ-deprotonated to form a delocalized ion along the glutarate-derived strand. We were also able to produce **3e** ($n = 12$) in a preparative-scale reaction in a biphasic mixture of dicholoromethane–THF with added aqueous NaOH. The isolated mixture of elimination products showed the expected additional vinylic signals required for **3e** in the ^{1}H NMR spectrum.

Scheme 3. Proposed competing hydrolysis and elimination of nitrophenyl phosphate during the membrane-spanning assay of Fig. 3A.

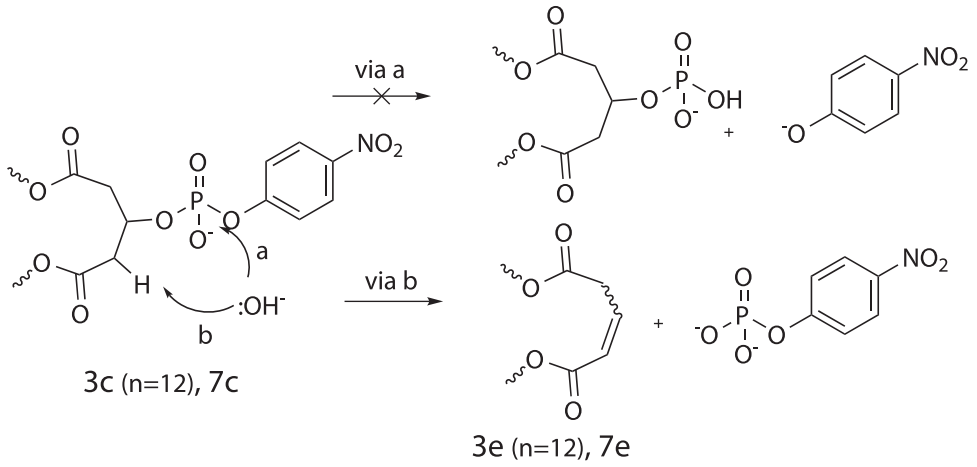

Although the logic of this (failed) assay is sound, it does have inherent ambiguities related to reaction rate relative to either lipid flip–flop or membrane permeation of the reagent. Another reaction that has been used in this context is the reduction of NBD-lipids by dithionite,[37,47–50] but this approach would suffer from the same ambiguities. As we thought about an alternative head group for the membrane-spanning proportion assay, we noted the early papers on the quenching of NBD-lipid fluorescence by Co^{2+} and Cu^{2+}.[47,51] Since a fluorescence-quenching assay would not require reaction time after initial mixing, this approach could potentially be faster and could provide an in situ probe for continuous monitoring of any competing processes, such as membrane permeation or lipid flip–flop. The proposed assay is sketched in Fig. 3B: an initially fluorescent vesicle population would suffer partial quenching on addition of the quencher to the outside of the vesicles. This would only be partial quenching dependent upon the quencher concentration according to a Stern–Volmer dependence. Upon vesicle lysis with a detergent such as triton, an additional fraction of the fluorescent head groups would be quenched. The proportion of membrane-spanning bolaamphiphiles would be related to the ratio of the extents of quenching. There are obvious complexities with such an assay. In the version developed, the main issue is that Co^{2+} quenching is known to be influenced by vesicle surface charge, and the vesicles themselves are unstable at high Co^{2+} concentration.[51] This requires the lowest possible quencher concentration, thus limiting the assay in the extent of the quenching that can be achieved. The analysis also needs to contend with the proportion of the signal that depends on the scattering of both incident and emitted light from the vesicles; any change to the vesicle morphology or population size distribution, such as provoked by addition of the detergent, has the potential to alter this factor and to confound the analysis of the signal and the ratios required for the determination of membrane-spanning proportion. Yet, even if these technical hurdles for fluorescence assay prove to be insurmountable, the dithionite reduction reaction-based assay remains as a potential back-up.

We therefore prepared NBD-labelled lipid cores **3d** (n = 14), **7d**, and **8d** as outlined previously. The synthetic NBD-lipids were handled as dilute solutions, with the concentration determined by UV–vis spectroscopy based on the assumption that the molar absorptivity of the NBD group was the same as that of **11** (λ_{max} = 475 nm; $\varepsilon = 1.82 \times 10^4$ L mol^{-1} cm^{-1}; $CHCl_3$). From a spectroscopic perspective, all three samples behaved the same as a commercially available NBD-lipid derived from distearoylphosphatidyl ethanolamine (NBD–DSPE). In particular, the absorbance and the emission spectra of **3d** (n = 14) were essentially superimposable on those of NBD–DSPE at the same concentration, whereas solutions of **7d** and **8d** appeared to be twice as concentrated but preserved the same absorption and emission maxima in $CHCl_3$ solution.

All four NBD-lipids were taken into vesicles comprised of egg phosphatidyl choline (70 wt%), cholesterol (25 wt%), a polyethyleneglycol-derivatized phosphatidyl ethanolamine (3 wt%), and egg phosphatidic acid (2 wt%). The NBD-lipids were added to a chloroform solution of the lipid mixture to give an NBD concentration of 0.08 mol% (about 0.1 wt% for **3d** (n = 14), the solvent was removed to form a lipid film that was hydrated in a HEPES buffer at pH 7.2, subjected to five freeze–thaw cycles, sonication, extrusion through a 0.1 μm nucleopore membrane, and gel-permeation chromatography to remove unbound materials. All NBD-lipids were obviously incorporated based on the pale yellow colour and the green fluorescence under hand-held UV light. The vesicles had the expected range of sizes between 125 and 200 nm mean diameter depending on the preparation. Excitation at 470 nm produced a clear fluorescence emission about 540 nm. The position of the emission maximum varied between 538 and 545 nm as has been previously ascribed to differences in the NBD location in the midpolar region, leading to changes in the contribution of water quenching to the observed emission.[47]

Addition of $CoSO_4$ quenched the NBD fluorescence of NBD–DSPC in vesicles. In the concentration range 10–50 mmol/L Co^{2+}, the plot of $(I_0/I - 1)$ as a function of Co^{2+} concentration is linear (r^2 = 0.9977, n = 5) with a Stern–Volmer quenching constant of 18.6 ± 0.5 (mol/L)$^{-1}$. This is in reasonable agreement with the reported value of 13.8 (mol/L)$^{-1}$ for the same NBD-lipid and Co^{2+} concentration range in a vesicle system composed of phosphatidyl serine and phosphatidyl ethanolamine (1:1).[51] However, the intercept of the linear fit is greater than zero, and the data below 10 mmol/L in Co^{2+} concentration are distinctly curved to zero. This behavior is similar to that observed in cases where there is restricted access to some of the fluorophores in the sample.[52] Compound **3d** (n = 14) behaves similarly; above 8 mmol/L Co^{2+}, the Stern–Volmer quenching constant is 15.7 ± 0.5 (r^2 = 0.9957, n = 7–40 mmol/L), with an intercept greater than zero. In the presence of triton in the same Co^{2+} concentration range, the Stern–Volmer quenching constant is essentially unchanged (16.3 ± 0.4, r^2 = 0.9976, n = 7–40 mmol/L), but the intercept is zero within experimental error (0.008 ± 0.009). In the very low concentration range of 0–0.2 mmol/L Co^{2+} without added triton, a linear fit produces an apparent Stern–Volmer constant of 215 ± 15 (mol/L)$^{-1}$ (r^2 = 0.98, n = 5). Whatever the photophysical origins of these behaviors might be, they have the positive practical consequence that sufficient quenching can be observed at 0.2 mmol/L Co^{2+} concentration to ensure that the quencher concentration lies well below the level at which transport and aggregation could be significant competitive processes.

As encouraging as these results were, there is a technical hurdle to overcome in that the addition of triton causes an apparent quenching of the emission. Figure 3C shows one example (**8d**) in which the addition of the detergent causes about the same extent of quenching as the addition of the quencher Co^{2+}. This may be due to a change in vesicle morphology that results in a change in light scattering, or it may reflect the influence of the detergent on the region where the NBD fluorophore resides that alters the extent of quenching by water.[47] As shown in Fig. 3C, the addition of Co^{2+} to vesicles already treated with triton results in additional quenching, shown previously to occur with the same efficiency as in the absence of the detergent. We reasoned that the Stern–Volmer factors ($I_0/I - 1$) in the absence of triton would be proportional to the fraction of NBD in the outer leaflet only, whereas the same factor in the presence of detergent would be proportional to the total NBD in the system. Thus, the ratio of the Stern–Volmer factors in the absence and presence of triton gives a measure of the proportion of the NBD head groups that lie in the outer leaflet. In the case of **3d** ($n = 14$), this ratio was 0.52 ± 0.03 for three trials from the same vesicle population. This is the expected value. As a dilute dopant, **3d** should be equally distributed in each leaflet, but the outer leaflet has a slightly larger area than the inner leaflet, which makes the outer area 53% of the total area (based on the experimentally determined vesicle diameter of 132 nm with an assumed 4 nm membrane thickness). We conclude that our procedure correctly estimates the outer leaflet proportion of NBD head groups.

The spectra obtained for similar experiments with vesicles containing the bolaamphiphiles **8d** (Fig. 3C) or **7d** "look" the same but differ significantly in the level of the head-group proportion apparently in the outer leaflet: **7d** gives an outer leaflet head-group proportion of 0.75 ± 0.03 and **8d** gives 0.48 ± 0.04. Note that the expectation value in both cases for a membrane-spanning bolaamphiphile is 50%, because the outer proportion does not depend on vesicle curvature. The experimental value for **8d** is clearly in line with the expectation that it adopts a membrane-spanning orientation as a low-level dopant in a predominantly phospholipid bilayer vesicle. The case of **7d** is much less clear: it is possible that it adopts a U-shaped insertion in a single leaflet of the phospholipid bilayer, but that would also require the assumption that it is predominantly located in the outer leaflet. There may be a lipid-packing argument to buttress this assumption, because the outer leaflet lipids occupy a larger area per molecule owing to curvature,[53] but this would be an unusually asymmetric distribution between the leaflets more commonly associated with small vesicles of higher curvature.[54] Alternatively, the U-shaped insertion might enhance the membrane permeability to Co^{2+} via defects as previously found in the synthetic ion channels area.[18–20] If permeation of Co^{2+} occurs, it could result in a time-dependent signal in the absence of triton. This was not observed in any experiment involving **3d** ($n = 14$), **7d**, or **8d** over time spans to 20 min, which suggests that the quenching behavior reaches a steady value within the mixing and sample preparation time (<1 min). Whatever the explanation, the conclusion from the experiments is that **7d** does not produce a solely membrane-spanning orientation at low concentration in phospholipid bilayers; if it did, it would have approximated the experimental result for **8d**.

Conclusion

The synthesis of a 72-membered macrocyclic tetraester bolaamphiphile was readily accomplished in a short sequence from commercially available starting materials using CuAAC. The 87% yield in the final macrocyclization step played a major role in the overall 26% yield in five steps to the lipid core diol. Subsequent losses occurred as phosphate head groups were appended, but the reported methods produce the macrocyclic lipids in acceptable overall yields. Lipids with two different phosphate head groups readily incorporated into phospholipid vesicles as directly detected in the NBD-lipid case or by ESI-MS analysis in the case of nitrophenyl phosphate lipids. Unfortunately, the latter failed to undergo phosphate hydrolysis under basic conditions but underwent elimination in competition; therefore, it could not be used to assay membrane-spanning proportion. The NBD-lipids produced allowed a new assay for membrane-spanning proportion to be explored based on the quenching of NBD fluorescence by cobalt ions. Apparent quenching in the presence of triton as detergent requires the comparison of the Stern–Volmer factors in the absence and presence of the detergent. The macrocyclic bolaamphiphile **8d** is incorporated into phospholipid vesicles such that 48% ± 4% of the NBD head groups are in the outer leaflet, consistent with a membrane-spanning orientation. There is no time-dependent change in quenching over 20 min, indicating that **8d** does not significantly alter the membrane permeability to the quencher or undergo lipid reorganization in this time scale. The acyclic bolaamphiphile **7d** is incorporated with 75 ± 3% of the NBD head groups accessible to quencher in the absence of a detergent suggesting U-shaped incorporation in the outer leaflet of the bilayer membrane and (or) some induced permeability of the vesicles by **7d**.

To what extent is the lipid core **8b** a mimic of the caldarchaeols? On a trivial level they both contain 72-membered rings and **8b**-derived lipids incorporate well into vesicles in a membrane-spanning orientation in line with the behavior of archaeal lipids. On the other hand, **8b** has completely different chemical functionality, and any presumed mechanical advantage of **8b**-derived lipids in stabilizing bilayer membranes has yet to be explored. In fairness, the functional role of the natural macrocycle is only indirectly inferred. All that can be stated at this point is that other derivatives of this mimic offer the potential to explore specific hypotheses and may lead to clarification of the roles of macrocyclic archaeal lipids.

Experimental

Synthesis

General procedure for preparation of glutarate monoesters: 2 and 4

In a two-necked round-bottom flask, a stirred solution in toluene (19 mL) was prepared from 3-(*tert*-butyl dimethylsilyloxy) glutaric anhydride (1.15 equiv.) and the alcohol (1.00 equiv.). The reaction mixture was set to stir at reflux for 24 h under a $CaSO_4$ drying tube. The reaction was monitored by thin layer chromatography (TLC) (silica gel, EtOAc/hexanes as eluent, visualized by $KMnO_4$). Once complete, the reaction was cooled, and toluene was evaporated at reduced pressure. The crude product was then redissolved in pentane, cooled in a dry ice / ethanol bath, and then vacuum filtered. Crystallization of excess anhydride from the filtrate was repeated until the excess crystals no longer formed. If alcohol impurities existed, as visualized by NMR, the crude product was purified by column chromatography on silica gel, using EtOAc/hexanes as eluent.

The following compounds were prepared by this procedure:

2 ($n = 12$) from 1-dodecanol (0.780 mL, 4.07 mmol) as a colourless oil in 95% yield (1.655 g). ^{1}H NMR (300 MHz, $CDCl_3$) δ: 4.54 (q, 1H, J = 6.0 Hz), 4.06 (dt, 2H, J = 1.5, 6.9 Hz), 2.70–2.55 (m, 4H), 1.64–1.26 (m, 20H), 0.90–0.87 (m, 12H), 0.10 (s, 3H), 0.09 (s, 3H). ^{13}C NMR (75 MHz, $CDCl_3$) δ: 177.0, 171.1, 67.9, 66.2, 64.8, 42.5, 42.4, 32.0, 29.7, 29.6, 29.5, 29.4, 29.3, 28.6, 26.0, 25.7, 22.7, 17.9, 14.1, –4.87, –4.92. ESI-MS (–ve): calcd for $C_{23}H_{45}O_5Si$ ($M–H^-$): 429.304 amu; found: 429.306 amu.

2 ($n = 14$) from 1-tetradecanol (1.140 g, 4.665 mmol) in 53% yield (1.397 g). ^{1}H NMR (300 MHz, $CDCl_3$) δ: 4.54 (quin, 1H, J = 6 Hz), 4.12–3.99 (m, 2H), 2.67–2.52 (m, 4H), 1.66–1.18 (m, 24H), 0.90–0.83 (m, 12H), 0.072 (s, 3H), 0.066 (s, 3H). ^{13}C NMR (300 MHz, $CDCl_3$) δ: 176.5, 171.0, 66.1, 64.8, 42.4, 42.2, 31.9, 29.65, 29.61, 29.54, 29.46,

29.3, 29.2, 28.5, 25.9, 25.8, 22.7, 17.8, 14.1, −4.9, −5.0. ESI-MS (–ve): calcd for $C_{25}H_{49}O_5Si$ ($M–H^-$): 457.366 amu; found: 457.374 amu.

4 from 10-undecyn-1-ol (1.49 mL, 7.77 mmol) in 87% yield (2.78 g). ^{1}H NMR (300 MHz, $CDCl_3$) δ: 4.54 (q, 1H, J = 6.0 Hz), 4.06 (dt, 2H, J = 6.9, 1.5 Hz), 2.7–2.54 (m, 4H), 2.19 (dt, 2H, J = 2.7, 6.9 Hz), 1.93 (t, 1H, J = 3.0 Hz), 1.25–1.66 (m, 14H), 0.86 (s, 9H), 0.09 (s, 3H), 0.08 (s, 3H). ^{13}C NMR (75 MHz, $CDCl_3$) δ: 177.0, 171.0, 84.6, 68.1, 66.1, 64.7, 42.4, 42.2, 30.3, 29.6, 29.3, 29.1, 28.9, 28.6, 28.5, 28.4, 25.8, 25.6, 18.3, 17.8, −4.9, −5.0. ESI-MS (–ve): calcd for $C_{22}H_{39}SiO_5$ ($M–H^-$): 411.256 amu; found: 411.257 amu.

General procedure for preparation of glutarate diesters: 3a and 7a

The glutarate monoester (1.0 equiv.) was dissolved in dry THF (15 mL). Under a flow of N_2, diisopropyl carbodiimide (1.5 equiv.) was added and stirred for 5 min. Hydroxybenzotriazole (1.5 equiv.) was then added and stirred for 5 min, followed by the alcohol (1.5 equiv.), which was stirred for 5 min, followed by diisopropyl ethyl amine (3.0 equiv.). The reaction was left stirring at room temperature (rt) for 3 h. The reaction was then vacuum filtered and the filtrate concentrated. The product was then dissolved in 50 mL DCM and extracted two times with H_3PO_4/NaH_2PO_4 buffer solution (50 mL, pH ~ 3), two times with Na_2HPO_4/NaH_2PO_4 buffer solution (50 mL, pH ~ 7), one time with water (50 mL), two times with 10% brine solution (50 mL), and finally washed once with a saturated solution of NaCl (50 mL). The crude waxy product was washed with MeOH, and the resulting solution was vacuum filtered. The MeOH wash was repeated as many times as necessary to increase purity as assessed by NMR with concomitant loss of yield.

3a (n = 12) from 1-dodecanol and **2** (n = 12) (1.270 g, 2.958 mmol) in 70% yield (1.238 g). ^{1}H NMR (300 MHz, $CDCl_3$) δ: 4.52 (q, 1H, J = 6.0 Hz), 4.06–4.01 (m, 4H), 2.52 (d, 4H, J = 6.3 Hz) 1.62–1.24 (m, 40H), 0.88–0.82 (m, 15H), 0.82 (s, 9H), 0.04 (s, 6H). ^{13}C NMR (75 MHz, $CDCl_3$) δ: 171.2, 66.5, 64.8, 42.7, 32.0, 29.8, 29.7, 29.6, 29.5, 29.4, 28.7, 26.1, 25.8, 22.8, 18.0, 14.2, −4.8. ESI-MS (+ve): calcd for $C_{35}H_{71}O_5Si$ ($M+H^+$): 599.5065 amu; found: 599.5065 amu.

3a (n = 14) from 1-tetradecanol (1.101 g, 2.399 mmol) in 59% yield (0.8524 g, 1.422 mmol). ^{1}H NMR (300 MHz, d_6-acetone) δ: 4.59 (quin, 1H, J = 6 Hz), 4.13–3.99 (m, 4H), 2.63–2.50 (m, 4H), 1.68–1.28 (m, 48H), 0.91–0.86 (m, 15H), 0.093 (s, 6H). ^{13}C NMR (300 MHz, d_6-acetone) δ: 171.4, 67.5, 65.0, 43.1, 33.9, 32.8, 30.5, 30.4, 30.1, 29.5, 26.8, 26.3, 23.4, 18.6, 14.5, −4.5. ESI-MS (+ve): calcd for $C_{39}H_{79}O_5Si$ ($M+H^+$): 655.569 amu; found: 655.565 amu.

7a from **6** (1.663 g, 1.694 mmol) and 10-undecyn-1-ol (0.780 mL, 4.06 mmol). The crude product was purified by column chromatography on silica gel, using EtOAc/hexanes as eluent, affording a colourless oil in 43% yield (0.930 g). ^{1}H NMR (300 MHz, $CDCl_3$) δ: 7.18 (s, 2H), 4.50 (q, 2H, J = 6.3 Hz), 4.42 (t, 2H, J = 5.1 Hz), 4.04–3.98 (m, 8H) 3.78 (t, 2H, J = 4.8 Hz), 2.65 (t, 4H, J = 7.8 Hz), 2.51 (d, 8H, J = 6.3 Hz), 2.14 (dt, 4H, J = 2.7, 6.9 Hz), 1.90 (t, 2H, J = 2.7 Hz) 1.64–1.22 (m, 56H), 0.80 (s, 18) 0.02 (s, 12H). ^{13}C NMR (75 MHz, $CDCl_3$) δ: 171.2, 148.6, 121.4, 84.8, 69.6, 68.2, 64.7, 50.0, 42.7, 29.6, 29.5, 29.4, 29.3, 29.25, 29.1, 28.8, 28.7, 28.5, 26.0, 25.9, 25.8, 25.76, 18.5, 18.0, −4.8. ESI-MS (+ve): calcd for $C_{70}H_{125}N_6Si_2O_{11}$ ($M+H^+$): 1281.894 amu; found: 1281.893 amu.

General procedure for tert-butyldimethylsilyl (TBDMS) deprotections: 3b, 7b, and 8b

The TBDMS-protected glutarate diester (1.0 equiv.) was placed in a round-bottom flask. TBAF (5.80 mL, 5.8 mmol, 5.0 equiv., from a 1.0 mol/L stock solution in THF) was added concurrently with AcOH (3.30 mL, 1.45 mmol, 1.25 equiv., from a 0.438 mol/L stock solution in THF). The solution was stirred under N_2 for 30 min at rt while being monitored by NMR. When the reaction was complete, it was quenched with a saturated NH_4Cl solution and DCM (25 mL) was added. The organic layer was washed with water (25 mL), brine (25 mL), and finally dilute acid (25 mL water, two drops HCl). The solvent was dried with Na_2SO_4, vacuum filtered, and the solvent removed under reduced pressure. The crude product was dissolved in pentane (25 mL) and crystallized in an ethanol / dry ice bath.

3b (n = 12) was prepared from **3a** (n = 12) (0.6900 g, 1.15 mmol) in 90% yield (502 mg). ^{1}H NMR (300 MHz, $CDCl_3$) δ: 4.44 (q, 1H, J = 6.3 Hz), 4.09 (t, 4H, J = 6.6 Hz), 3.41 (s, 1H), 2.53 (d, 4H, J = 6.3 Hz), 1.64–1.25 (m, 40H), 0.87 (t, 6H, J = 6.2 Hz). ^{13}C NMR (75 MHz, $CDCl_3$) δ: 172.0, 65.1, 64.9, 40.8, 32.0, 29.72, 29.67, 29.6, 29.4, 29.3, 28.7, 26.0, 22.8, 14.2. ESI-MS (+ve): calcd for $C_{29}H_{57}O_5$ ($M+H^+$): 485.4200 amu; found: 485.4199 amu.

3b (n = 14) was prepared from **3a** (n = 14) (0.248 g, 0.395 mmol) in 35% yield (0.0749 g, 0.139 mmol). ^{1}H NMR (300 MHz, $CDCl_3$) δ: 4.43 (quin, 1H, J = 6 Hz), 4.08 (t, 4H, J = 7 Hz), 2.53 (d, 4H, J = 6 Hz), 1.30–1.24 (m, 48H), 0.86 (t, 6H, J = 7 Hz). δ: 3.37–3.31 (m, 2H), 1.63–1.58 (m, 4H), 1.47–1.40 (m, 2H), 0.99 (t, 3H, J = 7 Hz). ^{13}C NMR (300 MHz, $CDCl_3$) δ: 171.8, 64.9, 64.8, 40.7, 31.9, 29.6, 29.52, 29.46, 29.3, 29.2, 28.5, 25.8, 22.6, 14.0. ESI-MS (+ve): calcd for $C_{33}H_{65}O_5$ ($M+H^+$): 541.483 amu; found: 541.484 amu.

7b was prepared from **7a** (271 mg, 0.211 mmol) as a white solid in 68% yield (152 mg). ^{1}H NMR (300 MHz, $CDCl_3$) δ: 7.16 (s, 2H), 4.40 (m, 6H), 4.03 (t, 8H, J = 6.8 Hz), 3.75 (t, 4H, J = 5.1 Hz), 3.52 (s, 2H), 2.62 (t, 4H, J = 7.5 Hz), 2.49 (d, 8H, J = 6.3 Hz), 2.11 (dt, 4H, J = 2.7, 6.9 Hz), 1.88 (t, 2H, J = 2.7 Hz), 1.58–1.24 (m, 56H). ^{13}C NMR (75 MHz, $CDCl_3$) δ: 171.8, 148.4, 121.4, 84.7, 69.5, 68.2, 64.9, 64.8, 49.9, 40.8, 29.5, 29.4, 29.3, 29.14, 29.13, 29.0, 28.7, 28.5, 25.8, 25.6, 22.7, 18.4. ESI-MS (+ve): calcd for $C_{58}H_{97}N_6O_{11}$ ($M+H^+$): 1053.721 amu; found: 1053.720 amu.

8b was prepared from **8a** (93.2 mg, 0.0638 mmol) as a white solid in 86% yield (77.2 mg). ^{1}H NMR (300 MHz, $CDCl_3$) δ: 7.21–7.17 (m, 4H), 4.43–4.46 (m, 10H), 4.08 (t, 8H, J = 6.9 Hz), 3.80 (t, 8H, J = 5.1 Hz), 3.54 (s, 2H), 2.67 (t, 8H, J = 8.1 Hz), 2.53 (d, 8H, J = 6.3 Hz), 1.13–1.63 (m, 56H). ^{13}C NMR (75 MHz, $CDCl_3$) δ: 172.0, 148.6, 121.5, 69.6, 65.0, 64.9, 50.0, 40.9, 29.6, 29.5, 29.4, 29.3, 28.7, 26.0,25.8. ESI-MS (+ve): calcd for $C_{62}H_{105}N_{12}O_{12}$ ($M+H^+$): 1209.796 amu; found: 1209.795 amu.

Copper-catalyzed azide–acetylene couplings: 6 and 8a

6 was prepared from **4** (1.612 g, 3.920 mmol, 1.99 equiv.) and DMAP (0.039 g, 0.32 mmol, 0.16 equiv.) dissolved in a stirred solution in DMF (32 mL). The azide 1,1′-oxybis(2-azidoethane) (**5**, 0.308 g, 1.97 mmol, 1.00 equiv.) was added, and the solution was degassed for 20 min with N_2, and then CuI (0.186 g, 0.977 mmol, 0.496 equiv.) was added. The flask was flushed with N_2, then sealed under a positive pressure of N_2 and stirred for 21.5 h at 12 °C. The reaction solution was diluted with DCM and washed with a saturated solution of disodium EDTA solution (50 mL) until the aqueous layer no longer remained blue. This was followed by two washes of water (50 mL) and two washes of dilute acid (50 mL, two drops of 1 mol/L HCl). In general, no purification was necessary. If excess azide was present (as determined by NMR), the partially reacted product was removed by dissolving the crude product in EtOAc (2 mL) and precipitated in hexanes (25 mL). The insoluble material was filtered and the filtrate was concentrated. Washes were repeated until no impurities remained. The reaction afforded a colourless, tacky semisolid that retained solvents that were removed on high vacuum. Compound **6** was a colourless oil afforded in 86% yield (1.667 g). ^{1}H NMR (300 MHz, $CDCl_3$) δ: 7.20 (s, 2H), 4.55 (q, 2H, J = 6.0 Hz), 4.46 (t, 2H, J = 4.8 Hz), 4.08 (t, 4H, J = 6.0 Hz), 3.81 (t, 2H, J = 4.8 Hz), 2.68 (t, 4H, J = 8.4 Hz), 2.61–2.58 (m, 8H) 1.66–1.25 (m, 28H) 0.85 (s, 18H), 0.09 (s, 6H), 0.08 (s, 6H). ^{13}C NMR (125 MHz, $CDCl_3$) δ: 175.0, 171.2, 148.5, 121.9, 69.5, 66.4, 64.8, 50.2, 42.8, 42.5, 29.6, 29.4, 29.3, 29.2, 29.1, 28.6, 26.0, 25.5, 18.0, −4.7, −4.8. ESI-MS (+ve): calcd for $C_{48}H_{89}N_6Si_2O_{11}$ ($M+H^+$): 981.6122 amu; found: 981.6121 amu.

8a was prepared from **7a** (0.371 g, 0.289 mmol, 1.00 equiv.) and DMAP (0.0025 g, 0.0020 mmol, 0.071 equiv.) in a stirred solution in DMF (2.550 mL) This was followed by 1,1′-oxybis(2-azidoethane) (0.0452 g, 0.289 mmol, 1.00 equiv.). Conditions and workup were as described for **6**. A colourless solid was afforded in 87% yield

(0.307 g) without the need for chromatography. ^{1}H NMR (300 MHz, $CDCl_3$) δ: 7.21–7.18 (m, 4H), 7.18 (s, 1H), 4.52 (q, 2H, *J* = 6.3 Hz), 4.44 (t, 8H, *J* = 5.1 Hz), 4.06–4.00 (m, 8H), 3.79 (t, 8H, *J* = 5.1 Hz), 2.66 (t, 8H, *J* = 7.8 Hz), 2.52 (d, 8H, 5.7 Hz), 1.66–1.23 (m, 56H), 0.82 (s, 18H), 0.04 (s, 12H). ^{13}C NMR (125 MHz, $CDCl_3$) δ: 171.24, 171.19, 148.58, 148.54, 121.51, 121.48, 69.62, 69.58, 66.5, 64.78, 64.75, 50.0, 42.7, 29.8, 29.64, 29.55, 29.43, 29.35, 29.3, 28.7, 26.0, 25.8, 18.0, −4.8. ESI-MS (+ve): calcd for $C_{74}H_{132}N_{12}Si_2O_{12}Na$ (M+Na$^+$): 1459.951 amu; found: 1459.9542 amu.

General procedure for nitrophenyl phosphate lipids: 3c, 7c, 8c

An oven baked round bottom flask was capped and cooled to rt under N_2 and 4-nitrophenyl phosphorodichloridate (**10**, 6.0 equiv.) was added, followed by dry DCM (700 μL) and pyridine (12 equiv.). The mixture was then stirred for 30 min. A second oven-baked round-bottom flask and condenser weres concurrently cooled under N_2 to rt and the alcohol (1.0 equiv.) was added, followed by dry DCM (100μL). The **10**/pyridine solution was added dropwise, and the mixture was stirred at rt for 30 min followed by 7.5 h at reflux. The reaction was cooled and Et_2O–H_2O (200 μL, 50:50) was added at 0 °C. Following vigorous overnight stirring, the yellow/orange precipitate in the round-bottom flask was isolated by decanting the supernatant and then dissolving the solid in DCM–MeOH (4 mL, 95:5). The product was precipitated from the solution with water (2 mL), and the precipitate was washed with dilute acid (2 mL H_2O, one drop HCl), and washed again with water (2 mL). The dissolution–precipitation cycle could be repeated as required. If necessary, the product was then adsorbed from DCM–MeOH onto silica gel, and a short column was done with DCM–MeOH as eluent to remove insoluble material, affording a yellow solid after solvent removal, usually with very significant losses on the column.

3c (*n* = 12) was prepared from **3b** (*n* = 12) (50 mg, 0.10 mmol) in 32% yield (22.6 mg). ^{1}H NMR (300 MHz, $CDCl_3$) δ: 8.14 (d, 2H, 9 Hz), 7.36 (d, 2H, *J* = 8.7 Hz), 5.16 (s, 1H), 3.98–3.95 (m, 4H), 2.82–2.66 (m, 4H), 1.51–1.22 (m, 40H), 0.87 (t, 3H, *J* = 6.3 Hz). ^{13}C NMR (125 MHz, $CDCl_3$) δ: 170.9, 125.5, 120.7, 65.7, 39.9, 32.1, 29.82, 29.76, 29.7, 29.50, 29.45, 28.58, 26.0, 22.8, 14.2. ESI-MS (–ve): calcd for $C_{35}H_{60}NO_{10}P$ (M–H$^-$): 684.3881 amu; found: 684.3865 amu.

7c was prepared from **7b** (95.5 mg, 0.091 mmol) in 17% yield (22.4 mg). ^{1}H NMR (300 MHz, $CDCl_3$) δ: 7.99 (d, 4H, *J* = 8.4 Hz), 7.17 (s, 4H), 5.13 (s, 2H), 4.84–4.45 (m, 4H) 4.11–4.04 (m, 12H), 2.68–2.54 (m, 12H), 2.16 (dt, 4H, *J* = 2.7, 6.9 Hz), 1.92 (t, 2H, *J* = 2.7 Hz) 1.64–1.22 (m, 56H). ^{13}C NMR (125 MHz, DMF-d_7) δ: 171.6, 148.4, 142.8, 125.9, 123.0, 121.2, 85.4, 71.0, 70.1, 65.1, 50.5, 40.8, 26.7, 18.9. ESI-MS (–ve): calcd for $C_{70}H_{102}N_8O_{21}P_2$ (M–2H^{2-}): 726.332 amu; found: 726.330 amu.

8c was prepared from **8b** (124 mg, 0.10 mmol) in 20% yield (33.0 mg). ^{1}H NMR (300 MHz, DMSO-d_6) δ: 8.108–8.083 (m, 4H), 7.59 (s, 4H), 7.32 (s, 4H), 4.74 (s, 2H), 4.41 (s, 8H), 3.82 (s, 8H), 3.74 (s, 8H), 2.71 (s, 8H), 2.53 (s, 8H), 1.52–1.19 (m, 56H). ^{13}C NMR (125 MHz, DMSO-d_6) δ: 170.0, 146.7, 124.9, 121.9, 119.9, 68.5, 63.8, 49.0, 29.0, 28.9, 28.71, 28.67, 28.6, 27.9, 25.3, 25.0. ESI-MS (–ve): calc'd for $C_{74}H_{110}N_{14}O_{22}P_2$ (M-2H^{2-}) 804.370 amu; found, 804.370 amu.

Elimination reaction: NMR sample of 3e

In a round bottom flask **3c** (15 mg, 0.022 mmol, 1.0 equiv.) was dissolved in DCM (2.5 mL), diluted with THF (20 mL), and 1 mol/L NaOH (145μL, 0.1 mmol, 7 equiv.) was added with stirring. After 4 h at rt, the reaction mixture was yellow and bleached when acidified with 1 mol/L HCl (6.0 × 10^1 μL, 0.06 mmol, 3 equiv.). Most of the solvent (~90%) was removed under vacuum, extracted with DCM (5 mL), and the organic layer was washed with water (5 mL), dilute acid (5 mL H_2O, one drop HCl), and again with H_2O (5 mL). The resulting product was chromatographed on silica gel with hexanes/EtOAc to produce a mixed products faction (~3 mg). ^{1}H NMR (300 MHz, $CDCl_3$) δ: 7.00 (dt, 1H, *J* = 7.2, 15.6 Hz), 5.93 (dt, 1H, *J* = 1.5, 15.6 Hz), 4.21–4.08 (m, 4H), 3.22 (dd, 2H, *J* = 1.5, 7.2 Hz), 1.64–1.259 (m, 40H), 0.87 (t, 3H, *J* = 6.3 Hz).

2-(7-Nitrobenzofurazan-4-yl)-amino-1-ethanol (11)

4-Chloro-7-nitrobenzofurazan (1.00 g, 5.01 mmol, 1 eq.) was heated in 35 mL methanol to fully dissolve the solid. A solution of 2-aminoethanol (2.137 g, 34.99 mmol, 7 equiv.) in 8 mL of methanol was added dropwise, and the mixture was held at reflux for 3 h. Solvent was removed under reduced pressure to yield a dark orange oil (3.611 g). The product adsorbed on 25 g of silica, slurried in 35 mL 15% methanol in chloroform, and transferred to a silica column in the same solvent. Isocratic elution and evaporation gave a product containing trace ethanol amine, which was recrystallized (acetone–hexane) to give NBD–ethanolamine as a red-orange solid in 39% yield (0.4450 g, 1.985 mmol). UV–vis: λ_{max} = 475 nm, ε (475 nm, MeOH) = 18 200 L mol^{-1} cm^{-1}. ^{1}H NMR (300 MHz, d_6-acetone) δ: 8.52 (d, 1H, *J* = 9 Hz), 8.14 (br s, 1H), 6.52 (d, 1H, *J* = 9 Hz), 4.23 (br s, 1H), 3.94 (t, 2H, *J* = 5 Hz), 3.78 (br s, 2H).

General procedure for NBD-lipids: 3d, 7d, and 8d

Stock solutions: NBD–ethanolamine stock (0.56 g in 10 mL dry THF, 0.25 mol/L), $POCl_3$ stock (0.232 mL in 10 mL dry THF, 0.25 mol/L), pyridine–water stock (0.202 mL pyridine + 20 μL water in 10 mL dry THF, 0.25 mol/L).

To 2 mL THF at 80 °C under nitrogen was added NBD–ethanolamine stock (0.24 mL, 60 μmol) and $POCl_3$ stock (0.24 mL, 60 μmol). The mixture was stirred at reflux for 4 h and the alcohol (<10 μmol) dissolved in 0.2 mL dry THF was added. After a further 4 h at reflux, the stock pyridine–water (0.30 mL, 75 μmol) was added, and the mixture of solids and solution was allowed to reflux overnight. The mixture was cooled, solvents were removed under vacuum, and the solid mass was suspended in 1 mL of $CHCl_3$ for transfer to a small silica gel column (40 × 8 mm). Elution with $CHCl_3$ (4 mL) followed by 4 mL each of 0.5% and 1% MeOH in $CHCl_3$ mobilized an intensely fluorescent band that was collected and concentrated to provide a stock solution for vesicle experiments. The NBD concentration of the stock was determined by UV–vis spectroscopy assuming the extinction coefficient of the products was the same as the starting NBD–ethanolamine. TLC (silica, 10% MeOH in $CHCl_3$, R_f 0.35) established the presence of a single component in the product solution. ESI-MS (-ve; unit resolution) gave the expected molecular ions:

3d calcd for $C_{41}H_{70}O_{11}N_4P$ (M–H$^-$): 825.5, 826.5 (2:1 ratio); found: 825.5, 826.5 (2.2:1 ratio);

7d calcd for $C_{74}H_{108}O_{23}N_{14}P_2$ (M–2H^{2-}): 811.36, 811.86 (1.2:1 ratio); found: 811.25, 811.8 (1:1 ratio);

8d calcd for $C_{78}H_{116}O_{24}N_{20}P_2$ (M–2H^{2-}): 889.4, 889.9 (1:1 ratio); found: 889.3, 889.8 (0.8:1 ratio).

Vesicle experiments

Vesicle preparation procedures

A mixture of lipids in chloroform solution was evaporated in a pear-shaped flask and held at high vacuum overnight. The resulting lipid film was hydrated with buffer solution by vortex mixing until all of the lipid material was suspended. The mixture was subjected to three cycles of freeze–thaw (liquid nitrogen then warm water) to produce a mixture of vesicles. In some experiments, the mixture was additionally sonicated at 3 W using a probe sonicator (three cycles of 20 s at 50% duty cycle). The vesicle suspension was then sized through a 0.1 um nucleopore membrane 19 times (Liposofast, Avestin). The sized sample was filtered on a Sephadex G-25 gel column eluted with the buffer solution used in the preparation. The first few cloudy drops through the column were discarded, and the remaining cloudy fraction was diluted to a known volume with the buffer. Vesicle diameter was determined by dynamic light scattering on a Brookhaven Instrument using ZetaPALS particle sizing software. Vesicle solutions were stored at 5 °C and used within 24 h.

Nitrophenolate release assay

Vesicles were prepared from a mixture of L-α-phosphatidylcholine (50 mg) and **3c** (3.2 wt %), **7c** (1.5 wt %), or **8c** (1.3 wt %) in a buffer of 0.01 mol/L Na_3PO_4, 0.01 mol/L NaCl, with the pH adjusted to 6.4 using concentrated H_3PO_4; the initial dispersion was in 0.8 mL of buffer. Final dilution was to 5.0 mL (~10 mg/mL lipid). Average vesicle diameter: **3c**, 126 ± 6 nm; **7c**, 148 ± 11 nm; **8c**, 147 ± 10 nm; PDI in all cases ~ 0.15. In a typical experiment, 500 μL of the vesicle solution was transferred to a 2 mm × 10 mm quartz cell, 10 μL of 1 mol/L NaOH solution was added to the cell, which resulted in a solution with pH ~ 11.8. The cell was then transferred to a UV–vis spectrometer and absorbance at 400 nm was monitored over time. No experiment produced a significant absorbance change because of nitrophenolate release.

NBD-lipid fluorescence quenching assay

Vesicles were prepared from a mixture of lipids (15 mg) consisting of 70 wt% L-α-phosphadtidyl choline, 25 wt% cholesterol, 3 wt% DSPE–PEG (1,2-distearoyl-sn-glycero-3-phosphoethanolamine-*N*-[methoxy(polyethylene glycol)-2000] (ammonium salt)), 2 wt% L-α-phosphatidic acid, and **3c** (0.1 wt%;,0.08 mol%), **7c** (0.2 wt%, 0.08 mol%), or **8c** (0.2 wt%, 0.08 mol%) in a buffer consisting of 0.01 mol/L KCl, 0.01 mol/LHEPES buffer, and adjusted with NaOH to pH = 7.2; the initial dispersion was in 0.5 mL of buffer. Final dilution was to 1.00 mL (~15 mg/mL total lipids). Average vesicle diameter: **3c**, 132 ± 8 nm (PDI 0.37 ± 0.01); **7c** 193 ± 2 nm (PDI 0.13 ± 0.015); and **8c**, 182 ± 2 nm (PDI 0.14 ± 0.01).

In a typical experiment, an aliquot of the vesicle solution (100 μL) was added to buffer (2.0 mL) in a 1 cm × 1 cm quartz cuvette. The sample was magnetically stirred and temperature equilibrated (25.1 °C) for 2 min in the fluorimeter. Trial experiments established that 10 μL of $CoSO_4$ solution (70.7 mmol/L, final diluted concentration 0.2 mmol/L) was sufficient for signal quenching. After temperature equilibration, the aliquot of $CoSO_4$ solution was added, and the spectrum recorded between 500 and 600 nm (λ_{ex} = 470 nm). Vesicles were lysed with triton solution (5 w/v%, pH = 7.2, 25 μL), and the spectrum was again recorded. As described in the text, the reverse order of addition — triton solution before $CoSO_4$ solution — was also required to generate a complete series for analysis. The proportion of head groups in the outer leaflet was then given as $(I_0/I - 1)_{\text{no triton}} / (I_0/I - 1)_{\text{with triton}}$.

Supplementary data

Supplementary data are available with the article through the journal Web site at http://nrcresearchpress.com/doi/suppl/10.1139/cjc-2016-0252.

Acknowledgement

The ongoing support of the Natural Sciences and Engineering Research Council of Canada is gratefully acknowledged.

References

(1) De, Rosa, M.; Gambacorta, A. *Prog. Lipid Res.* **1988**, *27*, 153. doi:10.1016/0163-7827(88)90011-2.
(2) Sprott, G. D. In *eLS*; John Wiley & Sons: Chichester, 2011; p. 12. doi:10.1002/9780470015902.a0000385.pub3.
(3) Woese, C. *Proc. Natl. Acad. Sci. USA* **1998**, *95*, 6854. doi:10.1073/pnas.95.12.6854.
(4) Fuhrhop, J.-H.; Wang, T. *Chem. Rev.* **2004**, *104*, 2901. doi:10.1021/cr030602b.
(5) Beveridge, T. J.; Choquet, C. G.; Patel, G. B.; Sprott, G. D. *J. Bacteriol.* **1993**, *175*, 1191.
(6) Jacquemet, A.; Barbeau, J.; Lemiègre, L.; Benvegnu, T. *Biochimie* **2009**, *91*, 711. doi:10.1016/j.biochi.2009.01.006.
(7) Chong, P. L.-G. *Chem. Phys. Lipids* **2010**, *163*, 253. doi:10.1016/j.chemphyslip.2009.12.006.
(8) Patel, G. B.; Sprott, G. D. *Crit. Rev. Biotech.* **1999**, *19*, 37.
(9) Brown, D. A.; Venegas, B.; Cooke, P. H.; English, V.; Chong, P. L.-G. *Chem. Phys. Lipids* **2009**, *159*, 95. doi:10.1016/j.chemphyslip.2009.03.004.
(10) Tolson, D. L.; Latta, R. K.; Patel, G. B.; Sprott, G. D. *J. Liposome Res.* **1996**, *6*, 755. doi:10.3109/08982109609039925.
(11) Sprott, G. D.; Dicaire, C. J.; Côté, J.-P.; Whitfield, D. M. *Glycobiology* **2008**, *18*, 559. doi:10.1093/glycob/cwn038.
(12) Sprott, G. D.; Yeung, A.; Dicaire, C. J.; Yu, S. H.; Whitfield, D. M. *Archaea* **2012**, *2012*, 513231. doi:10.1155/2012/513231.
(13) Eguchi, T.; Ibaragi, K.; Kakinuma, K. *J. Org. Chem.* **1998**, *63*, 2689. doi:10.1021/jo972328p.
(14) Delfino, J. M.; Stankovic, C. J.; Schreiber, S. L.; Richards, F. M. *Tetrahedron Lett.* **1987**, *28*, 2323. doi:10.1016/S0040-4039(00)96114-8.
(15) Markowski, T.; Drescher, S.; Meister, A.; Blume, A.; Dobner, B. *Org. Biomol. Chem.* **2014**, *12*, 3649. doi:10.1039/c4ob00048j.
(16) Fuhrhop, J. H.; Fritsch, D. *Acc. Chem. Res.* **1986**, *19*, 130. doi:10.1021/ar00125a002.
(17) Markowski, T.; Drescher, S.; Förster, G.; Lechner, B.-D.; Meister, A.; Blume, A.; Dobner, B. *Langmuir* **2015**, *31*, 10683. doi:10.1021/acs.langmuir.5b02951.
(18) Fyles, T. M.; Zeng, B. *J. Org. Chem.* **1998**, *63*, 8337. doi:10.1021/jo981195k.
(19) Moszynski, J. M.; Fyles, T. M. *J. Am. Chem. Soc.* **2012**, *134*, 15937. doi:10.1021/ja306596m.
(20) Fyles, T. M. *Acc. Chem. Res.* **2013**, *46*, 2847. doi:10.1021/ar4000295.
(21) Sakai, N.; Mareda, J.; Matile, S. *Acc. Chem. Res.* **2008**, *41*, 1354. doi:10.1021/ar700229r.
(22) Maccioni, E.; Mariani, P.; Rustichelli, F.; Delacroix, H.; Troitsky, V.; Riccio, A.; Gambacorta, A.; De Rosa, M. *Thin Solid Films* **1995**, *265*, 74. doi:10.1016/0040-6090(95)06620-9.
(23) Mathai, J. C.; Sprott, G. D.; Zeidel, M. L. *J. Biol. Chem.* **2001**, *276*, 27266. doi:10.1074/jbc.M103265200.
(24) Jacquemet, A.; Vié, V.; Lemiègre, L.; Barbeau, J.; Benvegnu, T. *Chem. Phys. Lipids* **2010**, *163*, 794. doi:10.1016/j.chemphyslip.2010.09.005.
(25) Drescher, S.; Lechner, B.-D.; Garamus, V. M.; Almásy, L.; Meister, A.; Blume, A. *Langmuir* **2014**, *30*, 9273. doi:10.1021/la501160s.
(26) Allen, T. M.; Cullis, P. R. *Adv. Drug Delivery Rev.* **2013**, *65*, 36. doi:10.1016/j.addr.2012.09.037.
(27) Wicki, A.; Witzigmann, D.; Balasubramanian, V.; Huwyler, J. *J. Controlled Release* **2015**, *200*, 138. doi:10.1016/j.jconrel.2014.12.030.
(28) Genge, K.; Moszynski, J. M.; Thompson, M.; Fyles, T. M. *Supramol. Chem.* **2012**, *24*, 29. doi:10.1080/10610278.2011.622382.
(29) Moszynski, J. M.; Fyles, T. M. *Org. Biomol. Chem.* **2010**, *8*, 5139. doi:10.1039/c0ob00194e.
(30) Fyles, T. M.; Luong, H. *Org. Biomol. Chem.* **2009**, *7*, 733. doi:10.1039/B816649H.
(31) Fyles, T. M.; Luong, H. *Org. Biomol. Chem.* **2009**, *7*, 725. doi:10.1039/b816648j.
(32) Eggers, P. K.; Fyles, T. M.; Mitchell, K. D. D.; Sutherland, T. *J. Org. Chem.* **2003**, *68*, 1050. doi:10.1021/jo026415f.
(33) Chui, J. K. W.; Fyles, T. M.; Luong, H. *Beilstein J. Org. Chem.* **2011**, *7*, 1562. doi:10.3762/bjoc.7.184.
(34) Fyles, T. M.; Hu, C.; Luong, H. *J. Org. Chem.* **2006**, *71*, 8545. doi:10.1021/jo0615753.
(35) Liang, L.; Astruc, D. *Coord. Chem. Rev.* **2011**, *255*, 2933. doi:10.1016/j.ccr.2011.06.028.
(36) O'Neil, E. J.; DiVittorio, K. M.; Smith, B. D. *Org. Lett.* **2007**, *9*, 199. doi:10.1021/ol062557a.
(37) Forbes, C. C.; DiVittorio, K. M.; Smith, B. D. *J. Am. Chem. Soc.* **2006**, *128*, 9211. doi:10.1021/ja0619253.
(38) Chui, J. K. W.; Fyles, T. M. *Org. Biomol. Chem.* **2014**, *12*, 3622. doi:10.1039/c4ob00480a.
(39) Pasini, D. *Molecules* **2013**, *18*, 9512. doi:10.3390/molecules18089512.
(40) Chouhan, G.; James, K. *Org. Lett.* **2011**, *13*, 2754. doi:10.1021/ol200861f.
(41) Schulz, M.; Tanner, S.; Barqawi, H.; Binder, W. H. *J. Polym. Sci., Part A: Polym. Chem.* **2010**, *48*, 671. doi:10.1002/pola.23820.
(42) Kuang, G.-C.; Guha, P. M.; Brotherton, W. S.; Simmons, J. T.; Stankee, L. A.; Nguyen, B. T.; Clark, R. J.; Zhu, L. *J. Am. Chem. Soc.* **2011**, *133*, 13984. doi:10.1021/ja203733q.
(43) Liu, X.-M.; Thakur, A.; Wang, D. *Biomacromolecules* **2007**, *8*, 2653. doi:10.1021/bm070430i.
(44) Moss, R. A.; Swarup, S. *J. Am. Chem. Soc.* **1986**, *108*, 5341. doi:10.1021/ja00277a047.
(45) Moss, R. A.; Li, J. M. *J. Am. Chem. Soc.* **1992**, *114*, 9227. doi:10.1021/ja00049a088.
(46) Moss, R. A.; Okumura, Y. *J. Am. Chem. Soc.* **1992**, *114*, 1750. doi:10.1021/ja00031a033.
(47) Chattopadhyay, A. *Chem. Phys. Lipids* **1990**, *53*, 1. doi:10.1016/0009-3084(90)90128-E.
(48) Balch, C.; Morris, R.; Brooks, E.; Sleight, R. G. *Chem. Phys. Lipids* **1994**, *70*, 205. doi:10.1016/0009-3084(94)90088-4.
(49) Boon, J. M.; Smith, B. D. *Med. Res. Rev.* **2002**, *22*, 251. doi:10.1002/med.10009.
(50) Angeletti, C.; Nichols, J. W. *Biochemistry* **1998**, *37*, 15114. doi:10.1021/bi9810104.
(51) Morris, S. J.; Bradley, D.; Blumenthal, R. *Biochim. Biophys. Acta, Biomembr.* **1985**, *818*, 365. doi:10.1016/0005-2736(85)90011-2.
(52) *Principles of Fluorescence Spectroscopy*, 3rd ed.; Lakowicz, J. R., Ed.; Springer: New York, 2006. doi:10.1007/978-0-387-46312-4.
(53) Heimberg, T. *Thermal Biophysics of Membranes*; Wiley-VCH: Weinheim, 2007.
(54) Israelachvili, J. N.; Marčelja, S.; Horn, R. G. *Q. Rev. Biophys.* **1980**, *13*, 121. doi:10.1017/S0033583500001645.

Copyright of Canadian Journal of Chemistry is the property of Canadian Science Publishing and its content may not be copied or emailed to multiple sites or posted to a listserv without the copyright holder's express written permission. However, users may print, download, or email articles for individual use.